

An Investigation of Head-Sea Parametric Rolling and its Influence on Container Lashing Systems

William N. France,¹ Marc Levadou,² Thomas W. Treacle,³ J. Randolph Paulling,⁴ R. Keith Michel,⁵ and Colin Moore⁵

Recent studies have demonstrated that parametric roll in extreme head or near head seas can occur when unfavorable tuning is combined with low roll damping (reduced speed) and large stability variations (governed by wavelength, wave height, general hull form, bow flare, and stern shapes). Parametric rolling is an unstable phenomenon, which can quickly generate large roll angles that are coupled with significant pitch motions. The rolling occurs in phase with pitch, and on containerships introduces high loads into the containers and their securing systems. It appears that post-Panamax containerships may be particularly prone to this behavior. This is an important issue considering the large number of these vessels scheduled for delivery in the next few years.

In October, 1998, a post-Panamax, C11 class containership encountered extreme weather and sustained extensive loss and damage to deck stowed containers. The motions of the vessel during this storm event were investigated through a series of model tests and numerical analyses. These studies provide insight into the conditions in which post-Panamax containerships are likely to experience head sea parametric rolling, and the magnitude of motions and accelerations that can occur. The findings from this investigation are presented in this paper, together with discussion of how such extreme motions impact the design and application of container securing systems. Also outlined in the paper are recommendations for additional research needed to better understand the influence of vessel design and operational considerations on the propensity of post-Panamax containerships towards parametric rolling.

Introduction

In late October 1998 a laden, post-Panamax, C11 class containership, eastbound from Kaohsiung to Seattle, was overtaken by a violent storm in the north Pacific Ocean. The encounter with the storm continued for some 12 hours, mostly at night, during which the master reduced speed and attempted to steer into increasingly higher seas off the vessel's starboard bow. Ultimately, the seas became completely confused and violent. Officers reported green water at bridge level during the worst of the storm and observed that container stacks immediately forward of the bridge had collapsed. The after bay of containers was also believed to have collapsed when a container corner casting punctured the main deck in the steering gear compartment allowing the ingress of seawater.

More significant than the violence and magnitude of the seas, however, were reports by experienced engine and deck officers of unexpectedly extreme and violent ship motions during the worst of the storm. At times yaw angles of 20 deg port and starboard made course keeping almost impossible. Main engine overspeed trips and shaft vibrations

together with pounding reflected significant pitch amplitudes. Port and starboard rolls as great as 35 deg to 40 deg were reported to have occurred simultaneously with the extreme pitching. The master later described the ship as absolutely out of control during the worst storm conditions.

When the crew surveyed the vessel the following morning they found devastation of the cargo. Of the almost 1300 on-deck containers, one-third, with their cargoes, had been lost overboard. Another one-third, with their cargoes, were in various stages of damage and destruction. Containers and cargoes hung over both sides of the vessel.

The vessel arrived in the U.S. to extensive news coverage and an army of surveyors and maritime lawyers. Wave impact damage could now be observed on forward container stacks from bow seas and along the entire starboard side from boarding seas. Surveys indicated that boarding seas had reached as high as the foremast and the running lights on the bridge. Cargo, container and vessel owners and their underwriters confronted the largest container casualty in history.

¹ Healy & Baillie, LLP, ² MARIN, ³ SAIC, ⁴University of Calif. (Ret), ⁵ Herbert Engineering Corp.



Figure 1 Representative Container Damage

C11 vessels have overall dimensions of LBP 262 m, B 40 m, D 24.45 m with a maximum summer draft of 14 m. The C11's are the second generation of post-Panamax containerships. The precursor class was designated C10 and had only slightly lesser dimensions, with a maximum draft of approximately 12.5 m. At the time of the events in late October 1998, the vessel's mean draft was 12.34 m, making the freeboard slightly more than 12 m. In the pre-casualty condition, the vessel's GM was approximately 2 m giving a natural roll period of 25.7 sec.

Pre-construction model tests of the C10 and C11 designs, in head and bow-quartering seas (of up to $H_s = 8$ m and $T_p = 15.0$ s) at speeds from 15 knots to slightly more than the design speed of 25 knots (and in beam seas at 0 knots), yielded maximum roll angles between 2.5 deg and 7 deg at a GM_t of 0.9 m.

Predictions by versions of the U.S. Navy Ship Motions Program (SMP) described in Meyers *et al.* (1981) at incremental relative wave headings through 360 deg predicted maximum roll angles of up to 30 deg in following and stern-quartering seas (of $H_s = 12$ m to 16m and $T_p = 15$ s to 21 s) at speeds between 20 knots and 24 knots and GM_t between 1.0 m and 2.5 m. In similar beam seas and for a similar range of GM_t , the predicted maximum roll was approximately 16 deg.

The roll motions excited by these model tests and predicted by the SMP calculations were normal synchronous rolling, which occur when the wave encounter period approaches the ship's natural roll period.

As a theoretical phenomenon, "auto-parametric" or, more briefly, parametric rolling has been known for many years. It has historically been of practical concern for smaller vessels of low or marginal stability in following seas. Roll response can be excited when the wave encounter period approaches one-half the natural roll period. In 1987, an early combined strip theory and time-domain ship motions

program at Institut für Schiffbau, Hamburg (SILAUF) was employed to study parametric rolling in following seas for the C10 design. Calculations were carried out at GM_t between 1.0 m and 3.0 m, speeds between 0 knots and 24 knots, and waves of up to $H_s = 15$ m and T_p 16.4 s. The calculations showed that roll angles of between 30 deg and 35 deg could be expected for the lower GM_t case ($GM_t=1.0$ m) at a 5 knot speed in following seas, when the wave encounter period was approximately one-half the natural roll period.

This sensitivity of containerships to heavy rolling in stern seas has been well studied, and the International Maritime Organization (IMO) has operational guidelines for masters on how to avoid dangerous situations in following and quartering seas (IMO, 1995). However, no model tests or time-domain motion computations were carried out for head sea parametric rolling for either the C10 or C11 designs. The phenomenon was not considered to be of practical concern in head seas.

Yet, in October 1998, here was a real C11 vessel in the north Pacific, steering into severe short-crested seas from forward of the beam to head seas that, according to her officers and crew, had experienced extreme angles of roll. Cargo and container losses and damage from this event gave rise to hundreds of claims which were consolidated in a Limitation of Liability action in the U.S. District Court in New York City. In the context of expert investigations in that litigation, the disparity between predicted and expected motions, on the one hand, and reported motions, on the other, became the impetus for the technical research reported in this paper.

The Storm Encounter and Hindcast

The vessel was weather-routed on her trans-Pacific voyage and also received regular reports and forecasts from the Japanese Meteorological Office and the U.S. National Weather Service. On departing Taiwan on 20 October, the routing service recommended way-points at 47° N, 175° E, then to 50° N, 165° W, and then to Seattle. The intention was to remain north of prevailing easterlies and south of the heaviest westerlies and swells associated with the dominant gale track for that season. The initial forecast on the route was NE to ENE winds of Beaufort 6-7, with waves of 3-4 m and swells of the same height.

However, on 24 October, the first recommended way-point was altered to the south and east, at 43° N, 180° E, to take the vessel below developing lows ahead of the vessel and also south of the predicted NE track of two lows developing behind the vessel. The vessel altered course accordingly. Even so,

severe conditions, with Beaufort 10 to 11 winds and combined waves and swell of 8.5 m to 11.7 m, were forecast for this track from late on 25 October through mid-day on 27 October.

The two developing and following lows were forecast to move NE'ly and to remain well behind the vessel's track. Within the next two days, however, the lows merged and developed into an "explosively intensifying low", or a meteorological "bomb". The storm also moved more easterly than predicted. By 26 October, 0000Z the storm's position had moved to within about 120 nm of the vessel. The vessel altered course further south, to 90 deg, at 0200Z in accordance with weather-routing recommendations. Seven hours later, the Master began a series of significant course alterations to the south accompanied by rpm reductions to ease increasing vessel motions as the region of highest wave heights moved directly over the vessel.

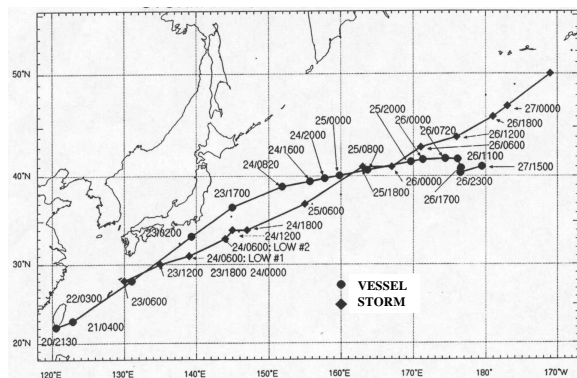


Figure 2 Vessel Track and Storm Track

The storm encounter continued until about 26 October, 1700Z, with the worst period of motions, including the extreme yaw angles and reported 35 deg to 40 deg rolls coupled with large pitch angles, between about 1300Z and 1430Z. The master testified that he tried to maintain the vessel's head into the prevailing seas, as best as he could determine, since the seas were completely confused. The deck log records winds of Beaufort Force 11 and sea state 9, the highest level on the International Sea State Scale, described as "phenomenal" and having average heights exceeding 14 m. As these events occurred at night when no one ventured outside the bridge and when the vessel's anemometer was not functioning, the deck log record of wind and wave conditions, as well as their relative directions, are only estimates.

To investigate the vessel's motions, a much more reliable description of seas and winds was required. Accordingly, a hindcast of conditions for the period 26 October, 0900-2000Z was commissioned. Meteorologists and oceanographers, Oceanweather,

Inc. and Dooley SeaWeather Analysis, Inc., employed a wave hindcast model termed the OceanWeather Inc. Third Generation Model (OWI3-G). This is a state of the art, well-documented hindcasting model based on a spectral energy balance equation, which equates the evolution of the wave spectrum to the sum of the local wind input, wave dissipation, nonlinear wave interaction and the propagation of non-local waves, or swell. All available data—buoy, vessel, coastal-marine automated stations, and satellite reports—were used by the model in an iterative process that included initial generation and kinematic reanalysis of wind fields using a marine planetary boundary layer model at three-hour intervals interpolated to hourly values. Resulting wind fields were input to the OWI3-G wave model over an array of 113 latitude grid points by 225 longitude grid points. At the vessel's position, grid points were spaced about 0.625° in latitude by 0.833° in longitude. The results were wave spectra (presented as a matrix of 24 directional zones and 23 frequencies) and properties (significant wave height, H_s , peak period, T_p , and vector mean direction, VMD) for all grid points.

The iterative process was repeated until hindcast H_s fell within 10% of the significant wave heights reported by the nearest polar orbiting satellites for the same times. Hourly spectra and wave properties were output for grid points surrounding the vessel's track. Additional processing interpolated these results to vessel GPS positions and separated spectra into sea and swell components.

Based on verification statistics of this model from its previous applications, the hindcast was estimated to have an H_s RMS error of about 1 m, a scatter index (the degree to which errors in predicted values scatter about the observed mean value) of about 18 percent, and a correlation coefficient of about 0.95.

After completion of the study hindcast, archived hindcast values from the National Center for Environmental Prediction (NCEP) which are based upon the Wavewatch III model having similar error statistics to OWI3-G, became available on the Internet. NCEP values were nearly identical with the hindcast study values at the vessel's locations. Later comparisons of U.S. Navy, NOAA and OWI3-G hindcast H_s with satellite values revealed that the OWI3-G results had the lowest RMS error and bias (tendency to over- or under-predict H_s).

According to the hindcast, for the 11 hour period considered, wind speeds at the vessel's positions ranged between 23.0 m/s (45 knots) to 30.8 m/s (60 knots) and about 29.5 m/s (57 knots) at the time of the most severe motions. Significant wave heights

steadily increased from 10.9 m with a T_p of 13.5 s at the beginning of the 11 hour period to 13.4 m and 15.4 s at the time of the most severe motions between hours 4 and 5.5 of the analyzed period. The maximum H_s was 14.9 m with a T_p of 16.4 s at hour 9.

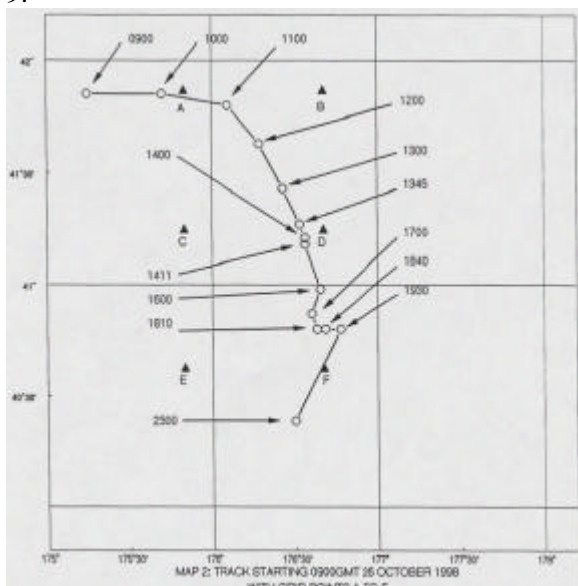


Figure 3 Vessel Track

GMT	Latitude (North)	Longitude (East)	Wind Speed (m/s)	H_s (m)	VMD (deg)	Peak Period (s)
0900	41.85	175.25	23.0	10.9	358	13.5
1000	41.85	175.70	24.0	11.1	004	13.8
1100	41.80	176.10	25.4	11.4	011	14.0
1200	41.63	176.29	27.0	11.9	023	14.3
1300	41.43	176.43	28.5	12.6	043	14.7
1400	41.21	176.56	29.5	13.4	045	15.4
1500	41.18	176.56	30.8	14.2	055	15.8
1600	40.98	176.65	29.8	14.6	064	16.2
1700	40.87	176.60	29.2	14.8	065	16.4
1800	40.80	176.63	28.2	14.9	070	16.4
1900	40.80	176.77	26.8	14.7	072	16.4
2000	40.39	176.50	23.4	14.3	075	16.4

Table 1 Hindcast Seastate (0900-2000Z)

A comparison of sea and swell VMD (the mean direction of waves during hourly intervals) with the vessel’s course recorder confirmed the master’s testimony that he had tried to keep the vessel’s head into the waves and that the relative direction of waves during the period of most severe motions varied between about 45 deg off the starboard bow to dead ahead and even off the port bow. It was estimated by those preparing the hindcast that the calculated VMD’s were likely to have an uncertainty of +/- 20 deg. Also, the actual direction of any individual wave crest would likely vary about the VMD due to the directional and frequency components of the energies of combining waves. Spectral results indicated that wave energy approached the vessel

from dead ahead and to either side of the bow at the time of the most severe motions.

Based on standard wave height distribution statistics, the expected maximum and extreme wave heights for an H_s of 13.4 m were 24.9 m (86.6 ft) and 32.1 m (105.5 ft). A climatological comparison of these conditions with data from the U.S. Navy Marine Climate Atlas for the North Pacific (1971), the U.S. Navy Spectral Ocean Wave Model (SOWM) Atlas for the North Pacific (1983) and Global Wave Statistics by N. Hogben, N. Dacunha and G. Oliver (1985), at similar north Pacific locations, revealed a frequency of occurrence of the most severe conditions likely to have been experienced by the vessel at between 0.0 and 0.1% for the month of October. It was also concluded that an encounter with the predicted extreme waves in this storm was not an expectable event during the vessel’s 25 year service life in the Pacific Ocean.

The hindcast spectra and properties were then utilized in the time-domain computer motion predictions using LAMP and FREDYN. Those data were also the basis for a matrix of wave heights and periods as well as direct input for the wave maker in MARIN’s new seakeeping basin where two series of vessel model tests were conducted during the spring and summer of 2000.

Occurrence and Characteristics of Auto Parametric Rolling Motion.

A transversely symmetrical ship moving in pure head or following long-crested seas will have motions of pitch, heave and surge, but will experience no transverse roll moment. Nevertheless, under certain conditions of encounter frequency, a rolling motion can exist. The roll motion, once started, may grow to large amplitude limited by roll damping and, in extreme conditions, may result in danger to the ship or its contents. This phenomenon is referred to as “auto parametrically excited motion” which is usually shortened to “parametric motion”. The term describes a state of motion that results not from direct excitation by a time-varying external force or moment but from the periodic variation of certain numerical parameters of the oscillating system. For a ship in head or stern seas the uneven wave surface together with the pitch-heave motion of the ship results in a time-varying underwater hull geometry. This varying geometry, in turn, results in time-varying changes in the metacentric height, i.e., in the static roll stability. The stability variations experienced by ship moving in longitudinal waves have been studied by a number of persons including Kempf (1938), Graff and Heckscher (1941) and Paulling (1959). W. Froude (1861), described a time-

varying transverse stability effect for a ship in regular beam waves which he ascribed to the variation in apparent weight density, therefore the pressure, of water particles surrounding the ship as it alternates between the trough and crest positions.

As a result of several casualties, involving fishing vessels and small coastal cargo carriers, most of the early attention to parametric motion and related phenomena was focused on following seas and low ranges of stability. Several of the early investigators, for example Paulling (1961), conducted both experiments and simplified computations that clearly illustrated the effect of waves and motions on transverse stability. In general, the stability variations are most pronounced in waves of length nearly equal to the ship length, and consist of an increase in stability (GM or righting arms) when a wave trough is near amidships and a reduction in stability when a crest is in this position. Figure 4 illustrates the variation of the righting arm curve for the C11 container ship in waves of length equal to the ship length and height of $L/20$. For these computations, the heave and trim attitude of the ship is assumed to correspond to static equilibrium, and this is approximately true for a low frequency of wave encounter as in following/overtaking seas. Head seas in which dynamic motions will be more pronounced will result in some modification to the righting arm curves but the general character will still be as shown in the figure.

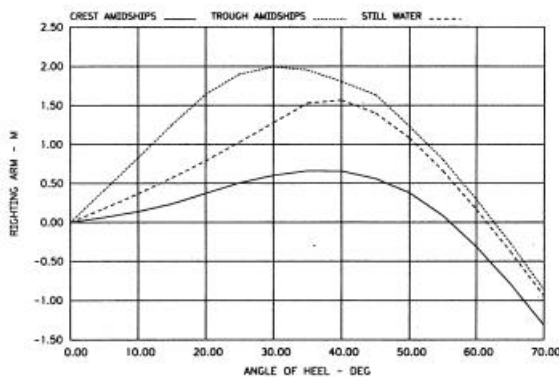


Figure 4 Stability curves for Post Panamax Container ship in L/20 Wave

The reason for this variation of stability with position of ship relative to wave profile can be seen by referring to Figure 6 which is an isometric view of the ship of Figure 4. When the forward and after sections are in successive wave crests with a trough amidships, the waterplane is, on average, wider than it is when in still water as a result of the flared section shape. This results in increased metacentric height and heeled righting moments compared to still water.

When the crest is amidships the mean waterline width, therefore the metacentric height and righting moments, are generally less because of the narrowing waterline at the ends and the stability is diminished compared to its value in still water.

Righting arm curves vary between the trough amidship and crest amidship values shown in Figure 4 as the waves move past the ship. In regular waves the righting moment will vary approximately sinusoidally with time between the extreme values. The single degree of freedom rolling motion of a ship in head or following seas may then be described by an equation of motion similar to that for still water. Now, however, the restoring moment is not only a function of angle of heel but it also varies sinusoidally with time. For small amplitudes of motion, we may use the small amplitude moment expression with a time varying metacentric height where the metacentric height equals the slope of the righting arm curve at the origin.

$$GM(t) = GM_o(1 + C \cos \omega t) \quad (1)$$

Here,

GM_o = still water GM

C = fractional variation of GM due to waves, heave and pitch

ω = frequency of variation of GM = frequency of encounter of waves

The equation of motion for small amplitude uncoupled roll motion without excitation is now given by Equation (2).

$$I_x \frac{d^2 \mathbf{f}}{dt^2} + \Delta \mathbf{f}(GM_o + CGM_o \cos \omega t) = 0 \quad (2)$$

Here,

\mathbf{f} = angle of roll,

$\ddot{\mathbf{A}}$ = ship displacement,

I_x = mass moment of inertia in roll, including added mass effect

Following Paulling and Rosenberg (1959), we divide both sides of (2) by I_x and make the change of variable, $\mathbf{t} = \omega t$

We note that $\omega_n^2 = \frac{\Delta GM_o}{I_x}$, where

ω_n = natural frequency of roll, and define

$$\mathbf{d} = \frac{\Delta GM_o}{\omega^2 I_x} = \frac{\omega_n^2}{\omega^2},$$

$$\mathbf{e} = \frac{C \Delta GM_o}{I_x \omega^2} = C \frac{\omega_n^2}{\omega^2},$$

the equation of roll motion now becomes,

$$\frac{d^2\mathbf{f}}{dt^2} + (\mathbf{d} + \mathbf{e} \cos t)\mathbf{f} = 0 \quad (3)$$

Equation (3) is recognized as the Mathieu Equation and is seen to be a linear differential equation with a time varying restoring coefficient. The solutions of this equation have been studied extensively and, of most interest to us here, are found to exhibit unstable behavior at certain values of the frequency parameter, \mathbf{d} . Figure 5 is the stability diagram for this equation. The shaded regions are stable corresponding to (\mathbf{d}, \mathbf{e}) pairs for which motion cannot exist and the unshaded regions are unstable, *i.e.*, motion can exist. If (\mathbf{d}, \mathbf{e}) lie in an unstable region, an arbitrarily small initial disturbance will trigger an oscillatory motion that tends to increase indefinitely with time. In a stable region, the initial disturbance will die out with time.

We see that δ is the square of the ratio of the natural frequency of roll to the frequency of the time varying GM, *i.e.*, the frequency of wave encounter, and ε is proportional to the fractional change in GM. The first unstable region is centered on a value $\delta=1/4$ or a ratio of natural frequency to frequency of GM variation of $1/2$. If the frequency of GM variation does not exactly satisfy this value, unstable motion can still occur if the value of the parameter of variation, C , is sufficiently large.

The effect of linear damping is merely to raise the threshold value of C at a given frequency of variation, ω . The unstable motion will still take place if C is sufficiently large and, in general, will grow without bound. In order for the motion to be limited in amplitude, there must be nonlinear damping present similar to quadratic or higher power of the roll velocity.

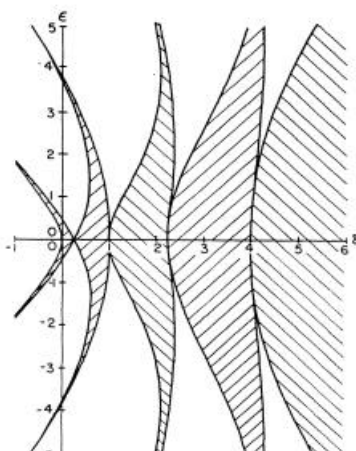


Figure 5 Stability Diagram for the Mathieu Equation

From the stability diagram, we see that unstable motion can occur at several different ratios of \mathbf{w}_r/\mathbf{w} . The predominant value of this ratio is $1/2$ meaning that oscillation at the natural frequency occurs if the frequency of encounter is twice the natural frequency. This instability phenomenon is an example of a dynamic motion “bifurcation”. That is, a situation in which either of two states of motion, zero or the growing oscillation, can exist depending on the absence or presence of an initial disturbance.

Equations (2) and (3) describe only the most elementary case of rolling in regular head seas. In the real world the situation is much more complex and the motion response includes, among other effects, those due to the nonlinear shape of the righting arm curve, nonlinear damping, cross coupling among all six degrees of freedom, and direct as well as parametric excitation of roll and other motions from wave components oblique to the ship. Research has taken two general directions. The first involves the application of classical methods of nonlinear dynamics, essentially an extension of the greatly simplified analysis represented by equation (1), and is exemplified by the work of Haddara (1973) and Dunwoody (1989a,b). The second, or simulation, approach involves the numerical solution of the nonlinear equations of coupled fluid and body motions, and at the highest level, this approach utilizes modern techniques of computational fluid dynamics. An early example with relatively simple fluid modeling is the work of Oakley et al (1974). This method was further developed by DeKat (1989) and resulted in the program KAPSIZE. More recent examples of this technique are implemented in the numerical procedures FREDYN and LAMP, results from which are presented in following sections.

The subject of head sea parametric rolling has been dealt with primarily in the academic and research communities. To date, it has not been recognized as a critical response requiring evaluation during the ship design process, and was not considered during the design of the C11.

Model tests conducted in the 1990’s demonstrated that large roll angles can be induced by head sea parametric rolling. Such tests were conducted on large cruise ships by Dalinga (1998), at MARIN, (the Maritime Research Institute in the Netherlands), and on naval replenishment ships at Virginia Tech by Oh *et al.* (1994).

From theory and as validated in these tests, parametric roll occurs when the following requirements are satisfied:

1. the natural period of roll is equal to approximately twice the wave encounter period
2. the wave length is on the order of the ship length (between 0.8 and 2 times LBP)
3. the wave height exceeds a critical level
4. the roll damping is low

The model tests demonstrated that hulls with wide, flat sterns and pronounced bow flare are susceptible to head sea parametric rolling. To induce large roll angles, the direction of the seas must be head to quartering head seas.

A rendering of the C11 hull form is presented in Figure 6. Typical of post-PANAMAX containerships, the C11 has extensive bow and stern flare.



Figure 6 C11 Hull Form

As previously discussed, the C11 that is the subject of this work encountered extreme waves during the 1998 storm. During this time, the master attempted to heave-to, or head the ship into the waves at reduced speed. Based on the hindcast study, the significant wave height H_s during the period of study ranged between 10.9 m and 14.9 m and the peak period T_p ranged between 13.5 and 16.4 seconds. The ship's natural roll period is estimated at 25.7 seconds. In head and quartering head seas, the ratio of the wave encounter period to the natural roll period (T_e/T_r) was close to 0.5 for speeds between 5 and 10 knots. The necessary conditions for parametric rolling during the 1998 storm were all in place.

Model Tests

The model tests performed on the post-Panamax, C11 containership were conducted in the new Seakeeping and Maneuvering Basin (SMB) at MARIN. The basin measures 170 x 40 x 5 m in length, width and depth respectively.

The basin is designed for tests with free-running models in waves from arbitrary directions. During the tests the main carriage follows the model over the total length of the basin. Below the carriage

mainframe, a sub frame spanning the full width of the basin follows the model in transverse direction.

At two adjacent sides of the basin segmented wave generators consisting of 331 hinged flaps are installed. Each flap is controlled separately making it possible to generate long-crested waves and short-crested waves, regular and irregular waves from any direction relative to the free sailing model.

Overview of test program

During the tests, the model had a draft of 12.339 m, a displacement of 76,318 MT, a GM_t of 1.973 m, and a natural roll period of 25.7 s. It was self-propelled at constant RPM and steered by means of an autopilot.

Wave Conditions

The main purpose of the model tests was to understand vessel motions during the storm encounter when extensive loss and damage of containers occurred. Secondly, the tests were conducted in order to gain an understanding of the influence of various factors on the vessel's roll response. The effects of speed, heading relative to the waves, wave height and wave period were investigated.

The tests were performed in wave conditions based upon the hindcast study and included regular waves and long- and short-crested sea conditions. One short-crested wave spectra was selected. A head sea direction and a bow quartering sea direction were used. The generation of the short-crested bow quartering was done with the actual hindcast data (both spectral shape and directional spreading). The spectra were measured at zero speed because no correction for forward speed is available for short-crested waves.

For the head sea condition, short-crested waves cannot be generated to match the hindcast spectrum. Rather, generation of short-crested waves in the longitudinal direction of the basin uses the "Dalrymple" method (Dalrymple, 2000) that relies on wave reflections from the longitudinal basin wall and the wavemaker along the opposite wall (which was not active during these tests). The result is a symmetric short-crested wave. The actual spectrum for head seas was approximated by a JONSWAP formulation with a peak enhancement factor γ of 1.39. For the directional spreading a cosine^m function with $m=3$ gave the best match with the hindcast spectrum, as indicated in Figure 7. For long-crested waves a JONSWAP spectrum with a peak enhancement factor γ of 1.39 was also applied.

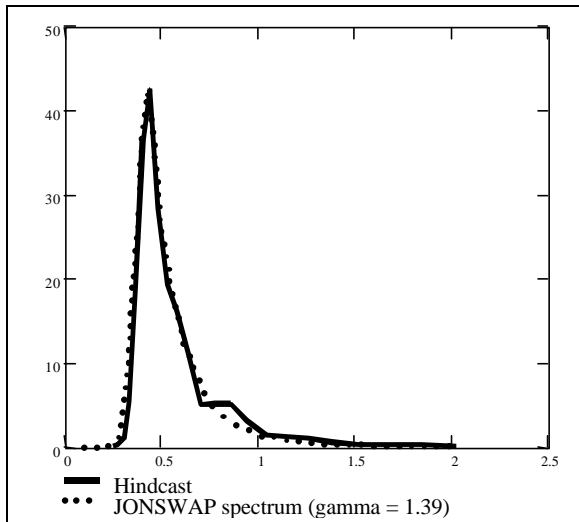


Figure 7 Comparison of Hindcast and JONSWAP Spectra

Presentation of model test results

An example of parametric rolling in regular waves from the model tests is presented in Figure 8.

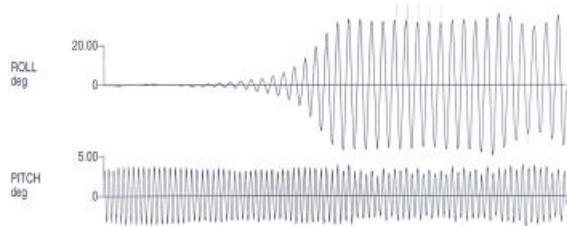


Figure 8 Roll and Pitch Motions

During 8 m Regular Waves (180 deg Heading – Head Seas)

As illustrated in Figure 8, the model was pitching to angles of about 4 deg, with negligible roll response. A small excitation, likely introduced by a rudder movement, causes the vessel to take a small roll to one side. Quite unexpectedly, roll angles then increased from a few degrees to over 30 degrees in only five roll cycles. This behavior is parametric rolling. Once parametric roll was initiated, the model continued to roll and pitch violently.

Figure 9 shows an expanded view of the roll and pitch response in regular waves. Positive pitch values mean the vessel is pitched down by the bow. It can be seen from Figure 9 that there are two pitch cycles for each roll cycle, and that the model is always pitched down by the bow at maximum roll. That is, when the model is at maximum starboard roll it is pitched down by the bow, when upright at zero heel it is pitched down by the stern, and when at

maximum port roll it is pitched down by the bow again. Throughout the test program, this relationship between pitch and roll motions existed whenever parametric roll was induced.

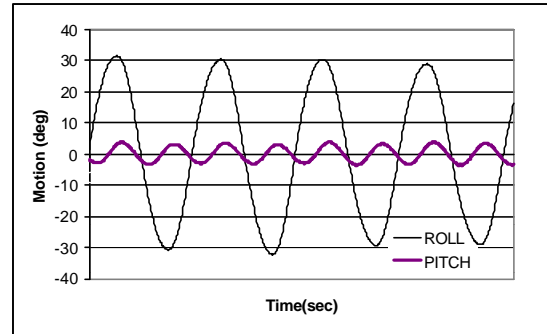


Figure 9 Expanded View of Roll and Pitch Motions During Regular Wave Test

Most of the irregular wave and short-crested sea tests fulfilled the requirements for parametric roll, as well. In Figure 10 the roll and pitch motions in way of the largest roll in short-crested seas are shown. The 2:1 ratio between roll period and pitch period is again apparent. When the model encounters a sequence of wave components of a certain period and height, parametric rolling is initiated. As in regular waves, the roll quickly builds to large amplitudes. When the wave period changes or the wave height diminishes, the parametric roll response quickly dissipates.

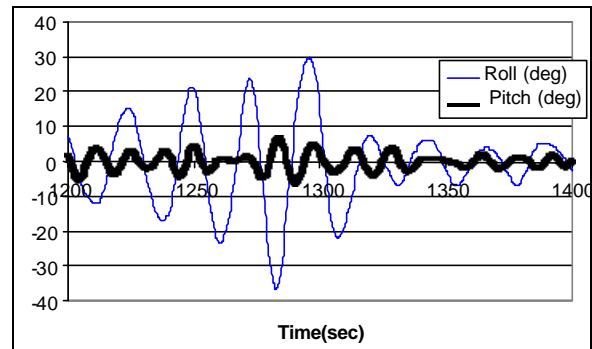


Figure 10 Expanded view of Roll and Pitch Motions at Time of Largest Roll in Short Crested Sea Test

During parametric roll, the model frequently immerses the main deck from amidships aft, as well as portions of the house. When pitching in the short-crested seas, green water is observed over the bow, impacting the forward-most bay of containers and the upper tier of the second bay of containers. This is consistent with the container damage observed on the vessel. The forward bay of containers was lost; the

containers in the upper tier of the second bay suffered impact damage; and containers and equipment along the starboard side aft were washed overboard or damaged.

In the Figure 11 results are given for the model tests performed in regular waves with a significant wave height of $H_s = 13$ m and a wave period of $T = 15.1$ s for a calm water speed of 16 knots. The wave heading was varied during these tests.

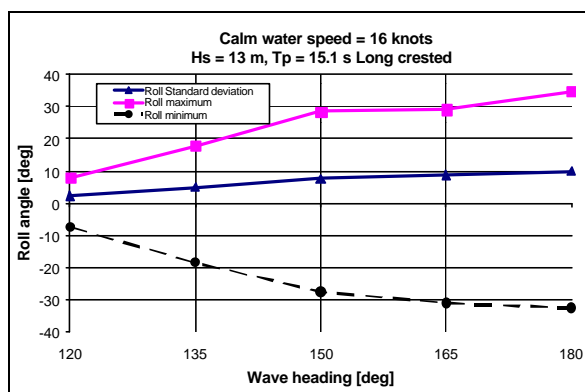


Figure 11 Influence of Heading on Roll Angle

The figures show the maxima and minima of roll angles as well as standard deviation. It can be observed that the heading has a large influence on the roll motion. Individual time traces of the tests show that parametric roll occurs at all headings (120 to 180 deg), although roll angles are much larger for bow-quartering (150 and 165 deg) and head sea (180 deg) conditions.

The higher roll excitation encountered in head seas is likely related to the wave shapes as they move along the ship and their influence on GM variations as shown in Figure 4. With a wave crest amidships and troughs at bow and stern, the waterline width amidships remains relatively unchanged due to the vertical vessel sides. However, the bow waterline width reduces significantly because of the V-shaped sections forward, and the stern waterline width reduces due to the flat and shallow sections aft. In quartering seas this effect is also present, but less pronounced than in head or following seas. Unless in resonance mode, the relative motions between wave surface and vessel sides in beam seas are small, causing relatively small variations in waterline width.

The influence of heading on roll angles is also influenced by sustained vessel speed. In Figure 12 the actual mean speed and speed standard deviation are given for the same tests.

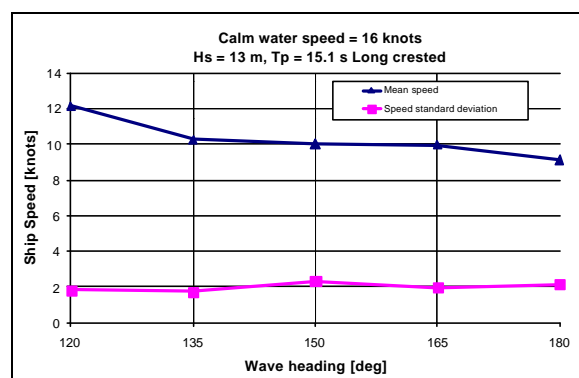


Figure 12 Influence of Heading on Speed

Speed is the mean speed during a test, also known as sustained speed. The difference between calm water and mean speed is due to the added vessel resistance in wind and waves. The influence of wave heading on mean speed can be seen in Figure 12. Speed decreases as the vessel approaches a head sea condition. Roll damping is dependent on speed and increases for higher speeds. In this case, bow seas result in lower speeds and thus lower roll damping, resulting in larger roll motions. This effect is also seen in the tests presented in Table 2.

Calm Water Speed (knots)	11	16	11	16	
Heading (deg)	180	180	180	180	
H_s (m)	14.50	14.50	12.63	12.63	
T_p (s)	16.20	16.20	14.65	14.65	
Seas	long-crested	long-crested	short-crested	short-crested	
Roll Angle:	StdDev (deg)	9.5	5.3	7.4	3.6
	Maximum (deg)	31.0	26.7	33.2	16.5
	Minimum (deg)	-30.4	-26.0	-33.6	-17.2
Speed:	Mean (knots)	8.1	10.3	5.2	10.1
	StdDev (knots)	2.2	2.0	1.4	1.5

**Table 2 Model Test Results
Influence of Speed on Roll Angle**

Two sets of tests were done in the same condition but with different calm water speeds. Firstly, it can be seen that the added resistance speed decrease is a greater percentage for low speeds (from 11 to 5.1 knots) than for high speeds (from 16 to 10.3). Secondly, roll angles are greater for lower speeds. Minimum and maximum roll angles are higher at lower speed as well as the roll angle standard deviation (more than twice as much). This indicates that within one test run there are more occurrences of parametric roll and that they also result in higher roll amplitudes.

To understand the relation between speed and roll angle it is necessary to analyze the model test results in more detail. The following example is for long-crested seas having a significant wave height of $H_s = 13.0$ m and wave period of $T = 15.1$ s, at a relative wave heading of 180 deg to the vessel. Calm water speed is 16 knots. In Figure 13 time series for

the test are shown for wave and roll amplitudes and vessel speed.

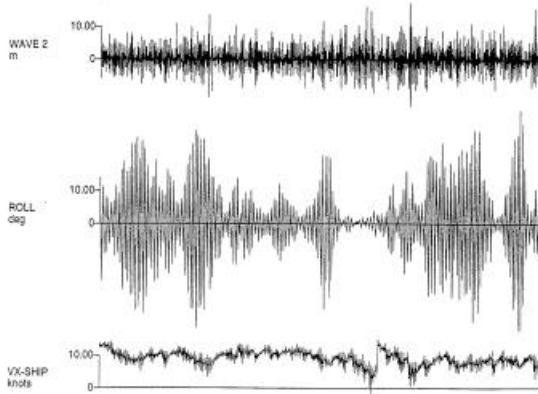


Figure 13 Model Test Results:
 $H_s = 13.0$ m, $T_p = 15.1$ s, Wave Heading = 180 deg
 and Calm Water Speed = 16 knots

In many of the instances of parametric roll a mean of the speed signal decreases before parametric roll begins. The reason for this effect appears to be that a group of high waves slows the vessel below a certain threshold speed allowing parametric roll to start. At that time added resistance increases due to loss of energy from higher roll amplitudes. This reduces the speed even more which allows even greater rolling until maximum roll angles are encountered. (Although this effect is not negligible it is assumed that it is smaller than the effect of the above mentioned wave grouping.) Parametric roll stops when excitation due to waves falls below a threshold value.

The relation between speed and parametric roll can also be seen in Figure 14 which is a scatter diagram of speed and roll angle combinations for the entire test run.

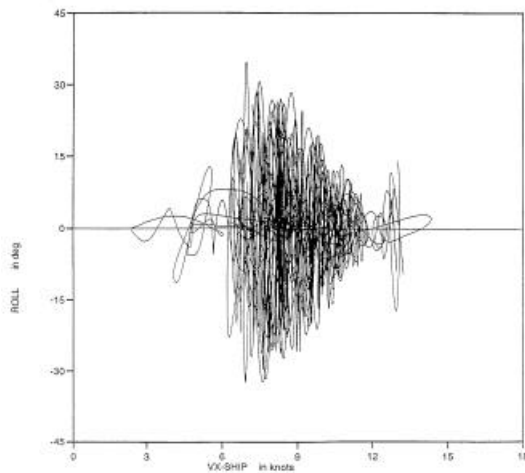


Figure 14 Speed – Roll Scatter Diagram

From the figure a clear relation between roll angle and speed can be seen. The lower the speed the greater the roll angles. Generally, with a sufficiently high speed, no large roll motions occur.

To assess the influence of speed variations on parametric roll, it is necessary to look at mean speed over several waves. The time series of the speed signal (Figure 13) shows a high frequency component oscillating about a low frequency component. The high frequency component is the effect of individual wave loads on vessel speed. The low frequency component is the mean speed over several wave encounters. The low frequency part and the high frequency part can clearly be seen in the speed spectrum of the same test (see Figure 15).

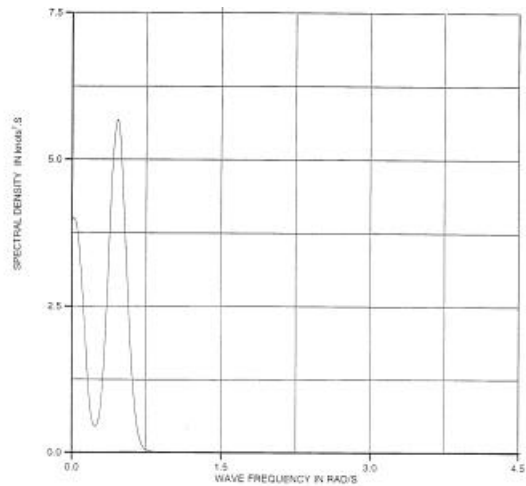


Figure 15 Speed Spectrum

Using the transition frequency as a low pass filter for the speed signal yields a low frequency speed trace. From that filtered speed trace a histogram showing the percentage of occurrences of a given speed during the test can be produced, as shown in Figure 16.

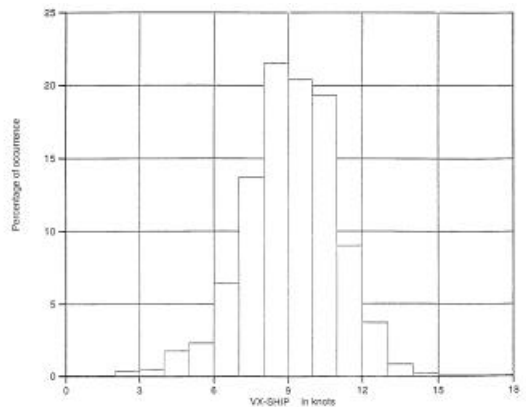


Figure 16 Speed Histogram

The histogram is broad, indicating a relatively large variation in speed during the test. The probability that a certain speed reduction occurs can be determined from the histogram. For example, it can be seen that the speed is under 7 knots for 11% of the time in the long-crested head sea conditions and at the calm water vessel speed of 16 knots utilized for this test.

In Figure 17 and Figure 18 two additional speed histograms are shown for tests in short-crested head seas with a wave height of $H_s = 14,5$ m and wave period of $T_p = 16.2$ s. One is for a calm water speed of 16 knots and the other for a calm water speed of 11 knots.

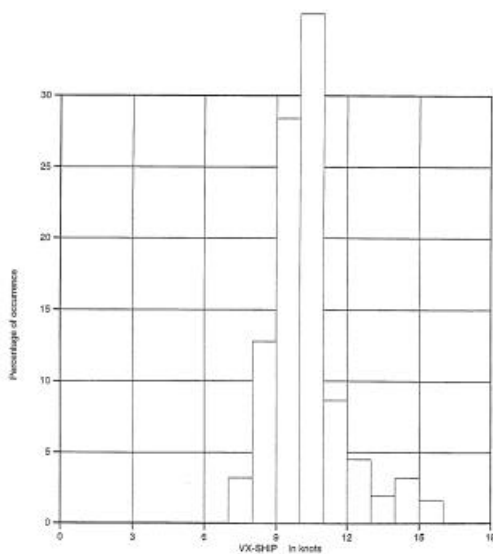


Figure 17 Calm water speed = 16 knots

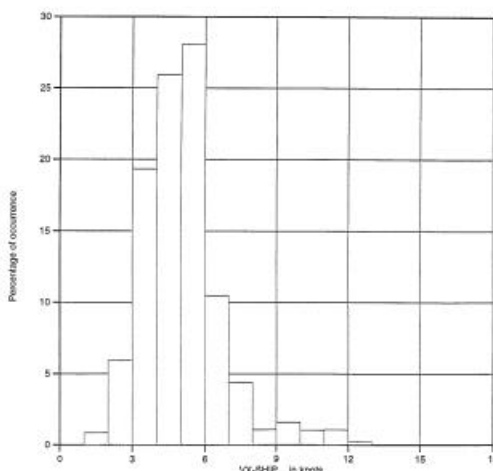


Figure 18 Calm water speed = 11 knots

The speed histogram for the lower calm water speed is wider. Besides the fact that lower speeds tend to increase the probability of parametric roll, a larger speed variation about a low mean speed will further increase that probability.

Assessment of Model Test Results

As previously discussed, parametric roll can occur when the vessel's natural roll period is approximately twice the wave encounter period, the wavelength is on the order of vessel length, wave height exceeds a certain critical level, and roll damping is low. However, the frequency of occurrence of parametric roll and the roll amplitudes also depend on the interaction of other factors.

From these model tests it can be seen that relative wave heading to the vessel has a large influence on the likelihood of parametric roll. As relative heading varies from beam seas, where no parametric roll response is observed, through bow quartering seas to head seas, both the frequency of parametric roll occurrences and roll amplitudes increase.

The model tests also show the influence of vessel speed on parametric roll. At lower speeds the frequency of occurrence of parametric roll is higher and the associated roll amplitudes are greater than at higher speeds. According to the model tests, the vessel speed must fall below a threshold speed before parametric roll occurs. Model test speed histograms are quite broad indicating that once parametric rolling is initiated it can continue at speeds even greater than the mean sustained speed.

Findings from Model Tests

- a) During the tests large roll motions and green water occurrences were observed. The impacts involved are consistent with the damage incurred on the vessel.
- b) Model tests made us aware of the magnitude of the speed variations due to the wave grouping and the influence it has on the probability of parametric roll.

Numerical Analysis using FREDYN

The FREDYN computer code (Hooft, 1987) was used to simulate ship motions for comparison with model test results. FREDYN is a nonlinear, time domain ship motion simulation program developed by MARIN over the last 10 years for particular use in predicting motions of naval frigates. However, it has also been utilized for commercial vessel motion predictions.

FREDYN takes into account the external forces on the ship due to wind and waves, rudders, bilge keels and active stabilizer fins and the reaction forces

of the ship due to the motions. The Froude-Krylov exciting forces are calculated up to the instantaneous waterline, which makes the program nonlinear. Since FREDYN is a full 6 degrees of freedom model it includes the couplings between the individual modes of motion. Both nonlinearity of the excitation forces and coupling between the 6 motions is required to be able to predict parametric roll motion. The maneuvering model is based on frigate type ships; all other routines are independent of the ship type. Since maneuvering was not a major aspect in this investigation, the FREDYN model was applicable.

FREDYN models a ship as a free sailing vessel in waves, comparable to a free sailing model in a seakeeping basin. The heading of the vessel is controlled by an autopilot that reacts on the instantaneous motions of the ship. The initial speed is set to the desired value and the RPM of the motor is set such that the ship sails the desired speed in calm water. Due to the waves, the speed and course of the ship change during the runs. However, different from MARIN's seakeeping basin, FREDYN is capable of modeling only uni-directional long-crested waves.

Description of analyses and comparison to model tests

FREDYN calculations were performed for a large number of combinations of headings, speeds and wave conditions. The same wave conditions were used as in the model tests except for the hindcast short-crested wave spectrum which cannot be input to FREDYN.

In the comparison presented here no tuning of the roll damping or speed was performed. From previous studies performed with FREDYN (Luth and Dallinga, 1998) it is known that when the roll damping is tuned with model tests results very good comparison of the roll motion can be achieved between model tests and the numerical analyses.

In Figure 19 and Figure 20 a comparison is shown between certain model tests and FREDYN results. The comparison is for the same wave headings, wave height and wave period although a calm water speed different from the model tests was used in the FREDYN calculation. Therefore, while a direct comparison of values is not possible, a comparison of speed trends with heading can be made.

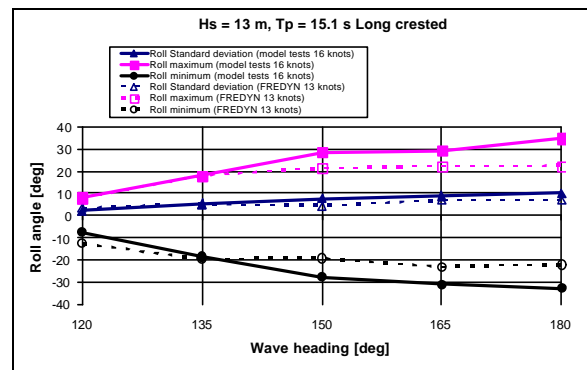


Figure 19: Comparison of Roll Response from FREDYN Analysis and Model Tests

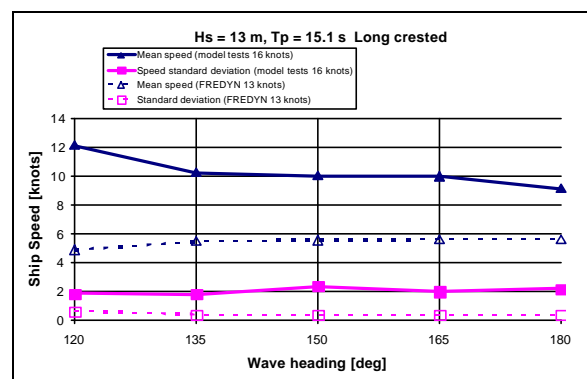


Figure 20: Comparison of Ship Speed from FREDYN Analysis and Model Tests

The roll angle comparisons show the standard deviations found by FREDYN and the model tests to be quite similar both in magnitude and trend. However, roll angle extremes are less well predicted by FREDYN. While the 120 deg and 135 deg heading results are nearly the same, FREDYN and model test results diverge at increasing relative headings, with greater roll angles from the model test results.

From the speed comparison figure, it can be seen that the mean sustained speeds from FREDYN and the model tests also differ. As mentioned, the calm water speeds for this comparison were different. However, it can also be seen that FREDYN does not predict the decrease in vessel speed due to added resistance in bow seas as was found in the model tests. This is the likely one of the explanation for FREDYN's prediction of lower roll angles in bow seas. Another explanation is the fact that the FREDYN calculations were done with a standard roll damping formulation. The roll damping was not tuned for a better comparison with the experimental results.

When FREDYN was run with long crested waves of significant wave height of $H_s = 13$ m and a calm water speed of 6 knots, the predicted maximum

roll amplitude is 42 deg. Running FREDYN at 6 knots simulates the expected slowdown from 11 knot calm water speed as determined in the model tests. In this case, the predicted roll of 42 deg is higher than the model test value of about 34 deg for the 11 knot calm water condition. Again, closer agreement can be expected if the roll damping is tuned for the FREDYN calculations.

Figure 21 and Figure 22 compare a portion of time traces from FREDYN calculations and model tests. Plotted are wave amplitude, roll angle and vessel speed.

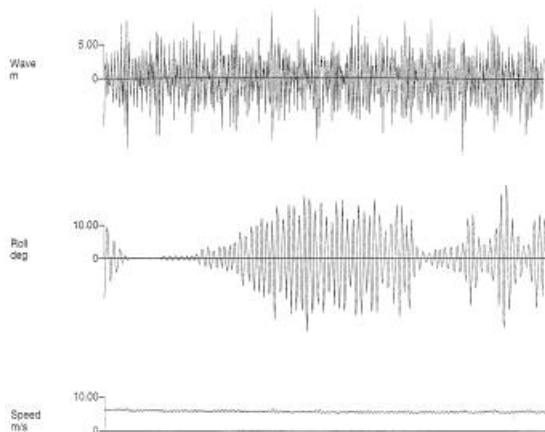


Figure 21: Results from FREDYN Calculations
 $H_s = 13.0$ m, $T_p = 15.1$ s, Wave Heading = 180 deg
 and Calm Water Speed = 13 knots

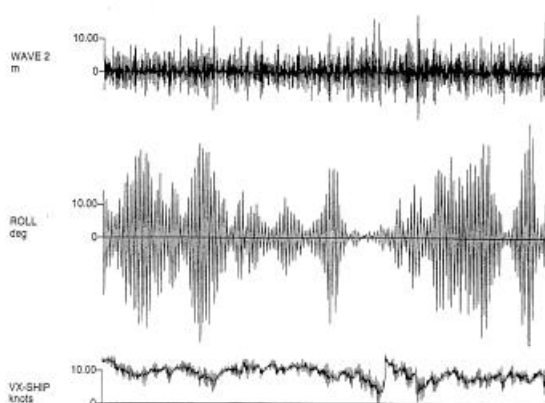


Figure 22: Model Test Results
 $H_s = 13.0$ m, $T_p = 15.1$ s, Wave Heading = 180 deg
 and Calm Water Speed = 16 knots

It can be seen that the parametric roll phenomenon is well predicted by FREDYN. Like the model test results, there is a period with no rolling and then, after an initial slight roll, amplitudes build rapidly to maximum values. However, FREDYN

does not accurately predict the speed variations found in the model tests which have a significant effect on parametric rolling.

Although FREDYN does not account for all hydrodynamic phenomena, the code is capable of predicting parametric roll in bow seas and can be used to predict if a vessel is likely to exhibit parametric rolling in an early design phase.

Findings From Numerical Analysis Using FREDYN

- FREDYN is capable of predicting parametric roll, although prediction of roll amplitude is of limited accuracy. Several important effects are not modeled by FREDYN—speed loss and speed variations—which likely account for this inaccuracy in amplitude.
- From other studies done with FREDYN (see Luth and Dallinga, 2000) it is known that nonlinear numerical simulation tools can give good results compared to model tests when the speed and roll damping are tuned.

Numerical Analysis Using LAMP

The LAMP (Large Amplitude Motion Program) System, Lin and Salvesen (1998), has been under development as a multi-level rationally-based time-domain simulation system for the prediction of motions, loads, and structural response for ships operating in extreme wave conditions. The LAMP System consists of several closely integrated modules. The first module is for the calculation of ship motions and wave-frequency loads. Other modules compute the slamming impact forces, green water on deck, and the whipping responses using a non-uniform-section dynamic beam method. The present studies used only the ship motion calculation module, which includes the calculation of body surface pressure distribution, local free surface elevations, rigid-body motions, and main girder loads. A constant forward speed setting was used in the simulations since the prediction of speed variations in extreme waves may not be adequately modeled in LAMP.

Series 60 Analysis

Through work under ONR Grant No. N00014-96-1-1123, an investigation of a Series 60 ship of block coefficient 0.7 in regular and irregular seas was performed. The purpose of the investigation was to identify the influence of above waterline geometry on the inception of parametric roll (as shown in Figure 23). Figure 24 shows a series of roll motion time histories calculated for Series 60 ships with different amounts of bow flare in irregular head seas. It can be

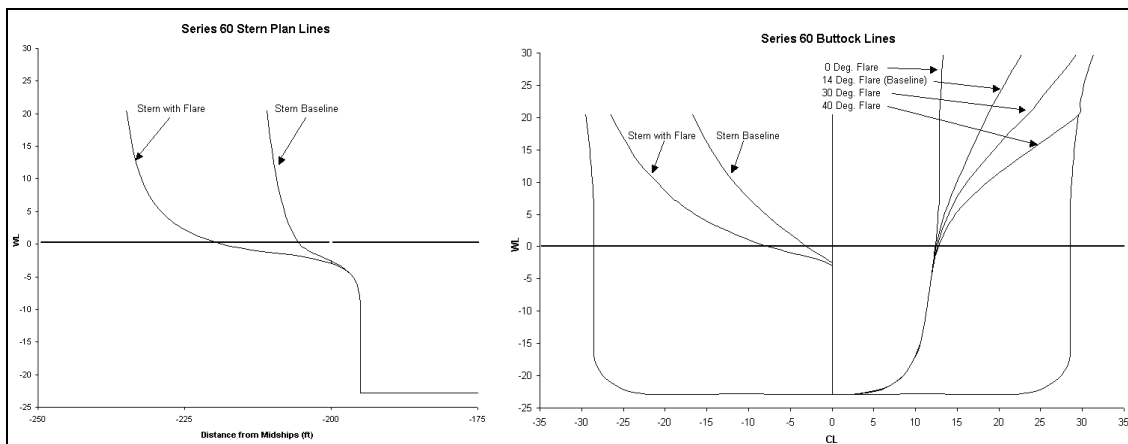


Figure 23 Geometry Variations for Series 60 Ship

seen clearly that the parametric roll phenomenon will occur when the bow flare is increased to 40 degrees. These results show that parametric roll is expectable and predictable. In addition, it seems that computations such as these can be used to provide practical guidance to ship operators for operating existing ships in severe conditions.

This study also confirmed that linear ship motion predictions such as LAMP-1 (linear formulation) or SMP cannot predict the parametric roll phenomenon as they do not account for geometry variation above the mean waterline. The investigation on the Series 60 ship also suggests that increasing damping through the use of large bilge keels and anti-rolling tanks (passive and active) can decrease the likelihood of parametric roll.

The Series 60 investigation illustrates the dependence of parametric roll on hull geometry characteristics such as bow flare and overhanging and flared sterns. Also, the trends and correlations found in this parametric roll investigation are consistent with our general understating of the phenomena:

- a) Head sea or near head sea wave encounter frequency is near twice the roll natural frequency.
- b) The incident wave must be above a threshold or critical amplitude for parametric roll to be initiated and sustained.

Parametric roll can occur over a fairly large range of encounter frequencies depending on the ship geometry and wave amplitude. The above water geometry, such as bow flare and overhanging sterns, has a significant impact on the bandwidth over which parametric roll can occur. A large bandwidth will also increase the likelihood of parametric roll in irregular seas as demonstrated in Figure 25.

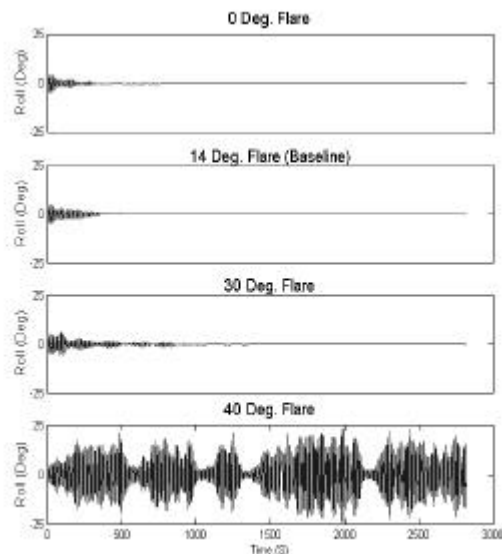


Figure 24 Effect of Bow Flare on Series 60 Ship in Long-crested Irregular Seas ($T_p = 11.2$ s, $H_s = 5.5$ m)

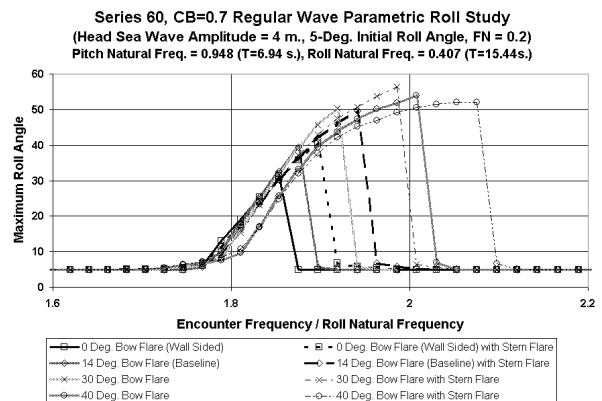


Figure 25 Effect of Geometry Perturbation on LAMP Computed Parametric Roll Domain

LAMP Calculations for C11 Containership

Several LAMP simulations for the C11-Class containership were performed for comparison to MARIN model tests. These simulations to investigate parametric roll were performed at the same load condition utilized for the MARIN model tests. The LAMP geometry is shown in Figure 26.

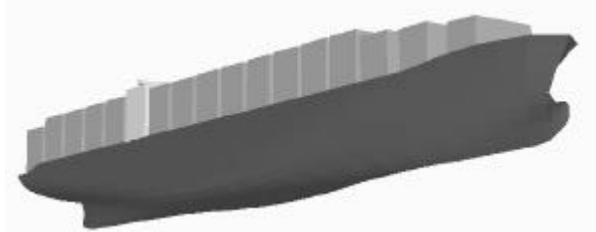


Figure 26 LAMP Geometry Definition of C11-Class Containership

Development of Roll Damping Model and Regular Wave Parametric Roll Responses

The magnitude of the roll response during parametric excitation is dictated in large part by the amount of viscous damping in the roll degree of freedom. To account for these damping effects in LAMP, an empirical roll damping model was established from the roll decay model tests at various speeds. The LAMP system does allow for several empirical ways to account for viscous roll damping with the default being an empirical method derived from the Kato (1966) methodology. For the C11 investigation, the LAMP-2 (nonlinear hydrostatics & linear hydrodynamics) roll decay response was tuned to match the experimental results by specifying an equation with up to cubic order terms of roll angle and roll velocity. The development of a nonlinear roll-damping model is critical for evaluating extremely large amplitude roll motions.

To verify the tuned roll-damping model in the LAMP System, comparisons to both roll decay tests and regular wave parametric roll tests were performed. The comparisons of roll decay coefficients between the tuned LAMP-2 simulations and roll decay tests at 5, 10, and 15-knots are shown in Figure 27. The roll and pitch motion comparison between the LAMP prediction with fixed forward speed and the full 6 degree-of-freedom experimental results in head regular waves are shown in Figure 28. The results in Figure 28 illustrate the accuracy of LAMP-2 in predicting the head sea parametric roll phenomenon in regular waves. The dependency of the roll magnitude on the type of roll damping model and the LAMP version used are shown in Figure 29, which has both the nonlinear tuned damping model and the Kato derived damping model. This figure also highlights the inability of a linear motion prediction system, such as LAMP-1, to predict the

parametric roll response even when using the Kato derived damping model, which tends to under predict roll damping for this type of ship.

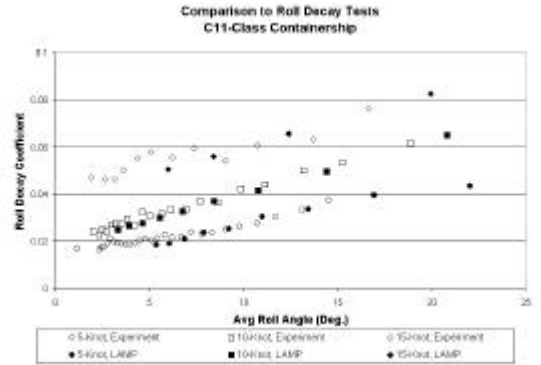


Figure 27 Tuning of Roll Damping for LAMP

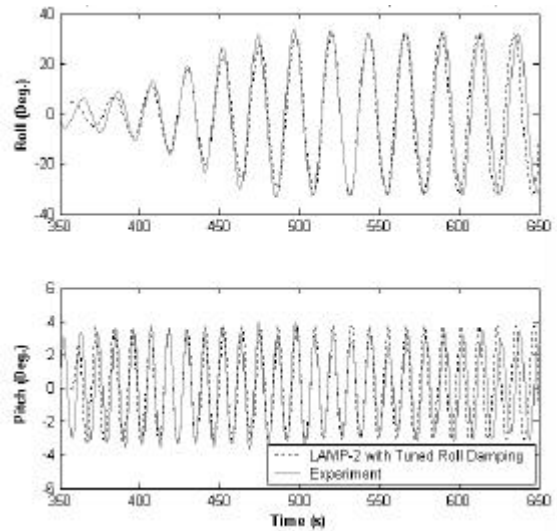


Figure 28 Regular Waves Comparison at 10 Knots ($T_{wave} = 14.0$ s., $H_{wave} = 8.4$ m)

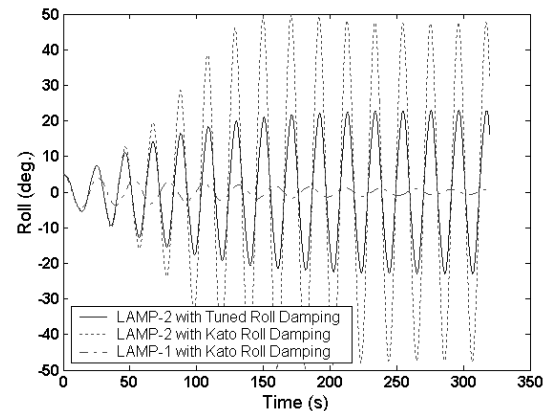


Figure 29 Effect of Roll Damping Model on Regular Wave Response ($T_{wave} = 14$ s., $H_{wave} = 8.4$ m)

Figure 30 shows the C11 response in regular waves of varying frequencies for the head sea condition. This figure illustrates the susceptibility of the C11 hull to parametric rolling over a wide frequency range like the previously discussed Series 60 ship with extensive bow flare and an overhanging flared stern. The width of the regular wave response curve suggests that the C11 hull form is likely to encounter parametric rolling in certain irregular seas.

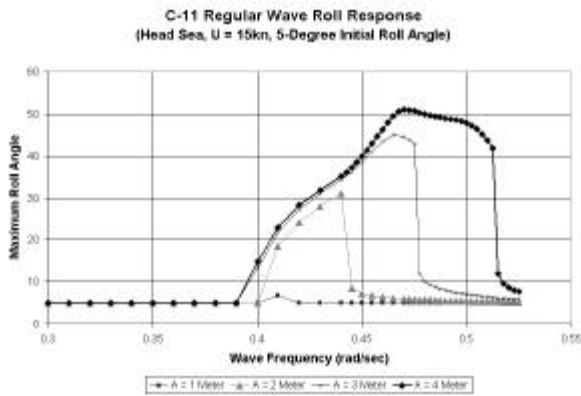


Figure 30 LAMP Regular Wave Parametric Roll Response for C11-Class Ship

LAMP Predictions of Parametric Roll in Short and Long Crested Seas

The LAMP system allows for the prediction of parametric roll in short-crested seas. For many years, it was thought that ships could not exhibit the parametric roll phenomenon in short-crested seas because the excitation forces were too broad banded. The LAMP roll-motion predictions shown in Figure 31 for a 7-knot forward speed in 5 degrees of freedom (fixed surge) show that this is not the case. For a severe short-crested seaway near a sea state 9 condition, the C11 encounters very significant parametric rolling. The seaway description in LAMP consists of superposing 376 individual wave components at 15-degree increments. The maximum roll angle encountered over the 1-hour LAMP simulation is 37.4 deg. This maximum roll angle is very close to the model test results observed in the MARIN tests.

The middle plot in Figure 31 shows a histogram of the individual roll motion cycles during the 1-hour LAMP short-crested seaway simulation. The lower plot in Figure 31 illustrates the variations in roll amplitude and period for each roll cycle. One would expect that the roll motion response would be localized near the roll natural period of 25.7 seconds. However for the C11-class ship, there is a large range of response periods for each cycle of roll motion while parametric roll events are occurring. The largest amplitude roll events tend to occur at periods

much shorter than the natural roll period. This period shifting is evidence of the nonlinear righting arm effect in the phenomenon and can be predicted theoretically. The large roll events tend to build very quickly and can have potentially serious consequences on a cargo-laden ship at sea.

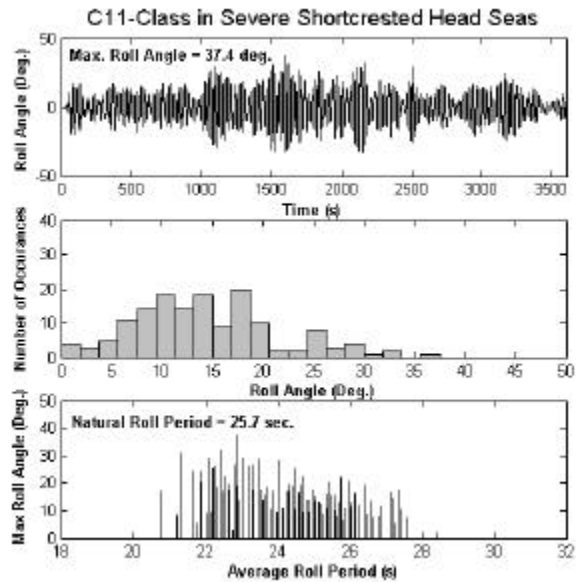


Figure 31 LAMP-2 Simulation for C11-Class Ship at 7-Knots in Severe Short-crested Head Seas

Direct comparison of motion time histories between the LAMP prediction and the model test results would be very difficult because wave events in short-crested seas are both space and time dependent. However, the linkage between maximum roll and bow down pitch observed in the model tests is also seen in the LAMP numerical simulation, as shown in Figure 32., which is an expanded view of the largest roll motion.

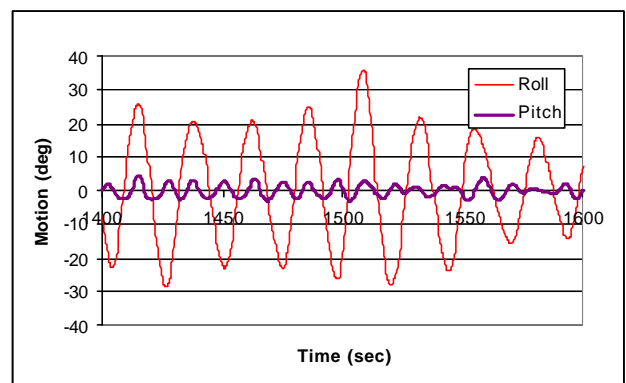


Figure 32 Expanded view of Roll and Pitch motions at largest roll (LAMP)

The parametric roll phenomenon is one that can occur in various sea conditions provided there is

sufficient encountered wave energy near twice the natural roll period. An operational polar diagram for long-crested seas in Figure 33 shows how large roll motions can occur over a wide range of speeds and headings for a given seaway/loading condition. The diagram is created from a series of LAMP simulations from 5 through 20 knots in 5-knot increments and 15 degree heading increments. All speed/heading combinations inside the shaded region exceed a 22.5-deg maximum roll angle during a 750-second simulation. The regions of higher speed and following seas correspond to a resonant roll condition where the pitch response frequency is near the roll natural frequency while the head sea regions are strictly parametric roll induced motions. While no simulations were performed for speeds less than 5 knots, the model tests indicate that parametric roll is also expectable at lower speeds. This type of diagram can be useful in helping a ship master avoid parametric roll while the ship is operating in severe sea conditions. It can also further the level of understanding of susceptibility to this phenomenon for a given hull form.

Lamp Predictions for C11 Containership
 Longcrested Seas ($T_p=14$ s, $H_s=12.6$ m)
 22.5 deg Max Roll Exceeded in Shaded Areas
 Operability = 0.352
 Head Seas

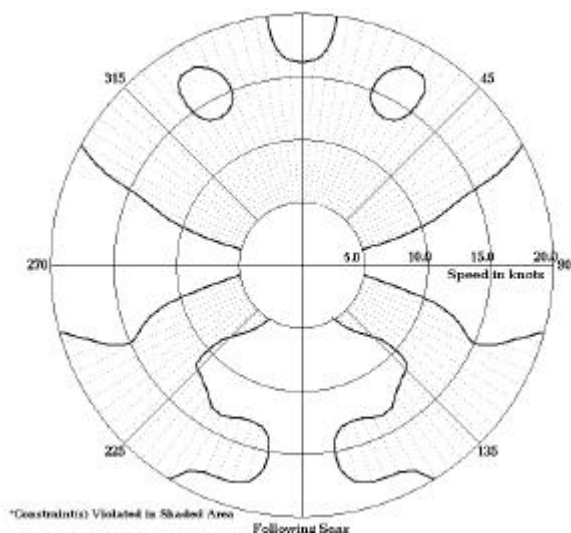


Figure 33 LAMP Operational Polar Diagram for C11-Class Ship in Long-crested Seas

Findings from Numerical Analysis Using LAMP

The LAMP System has shown its utility in the investigation parametric roll for both the Series 60 geometry variation study and the C11 Class ship investigation. The investigation findings show:

- a) An accurate estimation of the roll damping is essential for the exact prediction of the occurrence and magnitude of parametric roll.
- b) Above waterline geometry such as bow flare and stern shape have a significant effect on the propensity for parametric roll in irregular seas.
- c) Comparisons of regular wave roll response time histories between LAMP predictions and model test results were in very close agreement.
- d) The type of roll-damping model used in the LAMP simulation has a significant effect on the magnitude of roll response.
- e) The maximum roll angle seen in the short-crested head sea LAMP simulations with speed fixed to match model test average speed during parametric roll compared extremely well with the MARIN model tests when the hindcast spectrum was used.
- f) LAMP results shown in Figure 31 also illustrate that roll period shifting is evidenced in the prediction of the parametric roll phenomenon. Period shifting can be predicted theoretically as well as simulated with the LAMP System.
- g) The rapid build up of large roll events is predicted by LAMP.

Container Securing System Analysis

Deck container stacks on the C11 containerships are secured to lashing bridges, which are raised structures running athwartships between hatch covers. The lashing bridges enhance the effectiveness of the lashings, thereby increasing the weights of containers that can be carried. Unlike the Panamax designs, post-Panamax containerships are not stability limited and can take advantage of these higher stack weights. Lashing bridges were introduced on the first generation post-Panamax containerships, the C10 Class vessels built in Howaldtswerke-Deutsche Werft (HDW) during the mid 1980's, and have become a standard feature of current post-Panamax containerships. A brief description of the calculation methodology used to lash containers, both with and without lashing bridges, is described in the following paragraphs.

The forces acting on the containers are influenced by the motions of the ship, as well as wind loads on the sides of the containers. As explained in the following section, classification societies provide formulas for estimating these forces, or motions and accelerations can be determined from numerical simulation or model testing. When evaluating container lashing systems, the forces are typically resolved into normal-to-deck (vertical) and across-the-deck (transverse) components.

The transverse forces introduce racking loads across the ends of the container. These are partially resisted by lashings, and partially absorbed by the container. The stiffer the lashing, the greater the load absorbed by the lashing. The stiffer the container, the greater the load absorbed by the container. As the door end of a container is usually more elastic than the front end, calculations are carried out using both the door end and front end spring constants. Generally, the maximum lashing forces are encountered at the door end, whereas higher racking loads can be expected at the front end of the container due to its more rigid structure.

The forces and reactions acting on a deck lashed container stack are illustrated in Figure 34. The strength of the first tier container must be sufficient to resist the racking force R introduced into the top of the container. Likewise, the tension L in the rod lashing should not exceed the safe working load for the weakest component in the lash assembly.

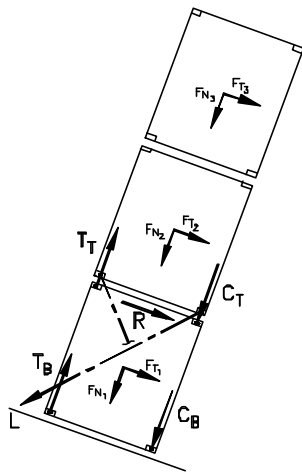


Figure 34 Reactions into Containers (with containers lashed to the hatch cover)

The transverse forces acting on a container stack also introduce a tipping moment. This tipping moment is partially resisted by the lashings, and partially by the twistlocks securing the containers to each other and to the base sockets. The upper tiers of containers pass loads into the top of the first tier container. The corner-post on the downhill side experiences a compression C_T , and the corner-post on the uphill side is normally subjected to a tension T_T . Similarly, a compressive force C_B acts at the bottom of the first tier container, distributing loads into the base socket and supporting structure. The tension T_B at the bottom of the container is resisted by the twistlock.

When the container stack is secured to a lashing bridge, the lashing typically extends to the bottom of the third tier container (see Figure 35). This

increases the effectiveness of the lashing in resisting the overturning of the container. Corner-post tension and corner-post compression reactions are reduced accordingly. Therefore, container stacks secured to the lashing bridge will generally have higher permissible weights.

The lashing bridge becomes less effective as the longitudinal distance between the lashing bridge and the container increases. This is most evident when stowing 40' containers in bays arranged for alternative 45' or 48' container stowage. As the ship distorts torsionally and the hatch cover slides closer to the lashing bridge, the lashings tend to slacken and absorb less load. Conversely, when the hatch cover slides further from the lashing bridge, the tension in the lashing assemblies increases.

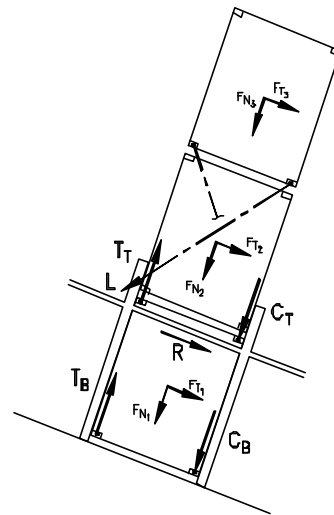


Figure 35 Reactions into Containers (with containers lashed to a lashing bridge)

Calculating the Forces Acting on Deck Stowed Containers

The maximum transverse accelerations acting on a container are usually introduced when the vessel is at an extreme roll angle. Maximum rolling normally occurs when the vessel encounters heavy beam or quartering stern seas. The loads in a deck stowed container stack and the associated lashing system are primarily influenced by the transverse force component, and therefore the maximum roll condition generally governs the design of the container securing system.

Maximum vertical and longitudinal accelerations acting on a container are usually developed when the vessel is at an extreme pitch angle. Maximum pitching occurs in head seas when roll motions are typically less significant.

Therefore, a resonant rolling condition in beam seas is frequently applied for assessing loads into the lashing system, and a head sea condition with extreme pitching is assumed when evaluating loads into the deck and hatch covers. This is the approach taken in the ABS “Guide for Certification of Container Securing Systems”.

As the first post-Panamax containerships, the C10 and C11 class vessels fell outside the bounds of prior experience, and therefore direct analysis rather than the classification society formulas was used to develop the forces acting on the containers. A frequency domain, strip theory program (ABS/SHIPMOTION) was used to develop RAOs, and long-term ship responses were predicted applying the H-family data for a probability level of 10^{-8} . Table 3 compares the calculated transverse accelerations used for determining permissible stack weights on the C11 class vessels with those calculated from the various classification society guidelines.

	C11 Longterm Analysis	ABS Lashing Guidelines	DNV Lashing Guidelines
Assumed max. GM	2.1 m	2.1 m	2.1 m
Roll Angle (degrees)	23.9	23.8	17.7
Across-the-deck accelerations			
6th tier	0.54 g	0.59 g	0.41 g
5th tier	0.53 g	0.58 g	0.40 g
4th tier	0.52 g	0.57 g	0.39 g
3rd tier	0.51 g	0.56 g	0.39 g
2nd tier	0.51 g	0.55 g	0.38 g
1st tier	0.50 g	0.54 g	0.37 g
Normal-to-deck accelerations			
Minimum	0.94 g	1.05 g	0.95 g
Maximum	1.05 g	1.15 g	1.00 g

Table 3 Comparison of Accelerations (per classification society guidelines)

The principal components of the overall transverse acceleration are gravity, tangential roll acceleration, and heave acceleration. Gravity is the dominant component. For instance, as determined by the ABS guidelines, the gravity component ($\sin 23.8$ deg or 0.40 g) comprises 75% of the total transverse acceleration of 0.54 g for the first tier container.

As illustrated in Table 3, the assumed maximum roll angles and therefore the maximum transverse accelerations applied by the different classification societies vary significantly. As the classification societies employ similar calculation methodologies and apply comparable factors of safety, the differences in computed accelerations are of concern as they translate directly into significant variations in the level of risk.

The Influence of Parametric Rolling in Head Seas on the Forces Acting on Deck Stowed Containers

In general, the C11 class vessels behave favorably in heavy seas. In beam seas, roll angles rarely exceed 15 deg. On a few occasions, roll angles between 25 deg and 30 deg have been encountered due to synchronous rolling in stern quartering seas, but the roll motions quickly dissipate with changes in course and speed. The tendency of containerships to roll in these conditions is well understood, and The International Maritime Organization has published guidelines for the master, for avoiding dangerous situations in following and quartering seas (IMO, 1995).

This operating experience is consistent with the model tests and numerical seakeeping analyses conducted during the design process of the C10 and C11 class vessels, which predicted significantly smaller motions than typically experienced with Panamax and smaller containerships.

When rolling in the resonant mode, a ship encounters one wave during one roll cycle. In the case of parametric roll, two waves pass the ship during one roll cycle. The ship rolls to one side when a wave crest is amidships, it is upright when the wave trough is amidships, and it rolls to the other side when the next wave crest is amidships.

A ship tends to roll close to its natural roll period whereas it tends to pitch at the wave encounter period. As documented in the previous sections of this paper, a vessel experiencing parametric rolling will go through two full pitch/heave cycles for each roll cycle. Unlike a ship rolling in beam seas, parametric rolling in head seas is accompanied by a significant pitch response. Each time the ship is at its maximum roll angle, it is concurrently pitched down by the bow. When a ship is pitched down by the bow, the normal-to-deck force acting on a container near the bow is increased. This, in turn, increases corner-post compression. Conversely, the normal-to-deck force acting on a container near the stern is reduced, and corner-post tension and the tensile load in the twistlocks increase.

In Table 4, the accelerations applied in the design calculations for the C11 vessel lashing system are compared to those derived from a MARIN model test at three stack locations. In this test, the hindcast wave spectra at the time of the container casualty was simulated. That is, short-crested seas with H_s of 12.63 meters and T_p of 14.65 seconds. The model, while heading into the predominant wave direction, underwent parametric rolling and recorded a peak roll of 36.8 deg. When adjusted for wind effects, the maximum roll angle is 40.1 deg. This is consistent with the roll angles of 35 to 40 deg which occurred

simultaneously with extreme pitch motions as reported by the vessel's officers.

The large roll amplitudes associated with parametric roll result in across-the-deck accelerations that are 33% to 80% higher than were anticipated. The large pitch component has a significant impact on the normal to deck accelerations aft. The normal-to-deck acceleration at bay 62 (the aft-most bay on the vessel) is less than one-half the value expected when the vessel and its securing system were designed. The effect is to substantially increase corner-post tension

Table 5 shows the contributions of the six degree of freedom motions to accelerations at a bay 62 stack. The total across-the-deck acceleration is -0.77 g. The gravity (-0.64 g), tangential roll (-0.12 g), and yaw (-0.03 g) acceleration components are all in phase, and contribute to the across-the-deck force acting on the container. The pitch is positive at maximum roll, and

therefore the bow is down at each peak roll, port or starboard. The overall normal acceleration is therefore smaller at the stern when the pitch component (-.033 g) is acting in the opposite direction as the gravity component. For this particular condition, the heave component (-.03 g) is also acting to reduce the normal-to-deck acceleration. The normal to deck acceleration of 0.48 g is observed when the pitch and heave components are acting opposite to the gravity component, and the roll is acting in the direction of gravity. The tangential roll component can make either a positive or negative contribution to the normal-to-deck force, depending on whether the stack being evaluated is to port or starboard of centerline. The stack under consideration is the port-most stack. If we consider the starboard-most stack, the roll acts against gravity and the normal-to-deck force is further reduced to 0.34 g.

	C11 Longterm Analysis	MARIN MODEL TEST 2310		
		Bay 62 Stack 12	Bay 38 Stack 14	Bay 2 Stack 08
Assumed max. GM	2.1 m	1.97 m	1.97 m	1.97 m
Roll Angle (degrees)	23.9	40.1	40.1	40.1
<u>Across-the-deck accelerations</u>				
6th tier	0.54 g	0.77 g	0.75 g	0.72 g
5th tier	0.53 g	0.75 g	0.74 g	0.70 g
4th tier	0.52 g	0.74 g	0.72 g	0.69 g
3rd tier	0.51 g	0.73 g	0.71 g	0.68 g
2nd tier	0.51 g	0.71 g	0.69 g	0.66 g
1st tier	0.50 g	0.70 g	0.68 g	0.65 g
<u>Normal-to-deck accelerations</u>				
Minimum	0.94 g	0.34 g	0.62 g	1.02 g
Maximum	1.05 g	0.48 g	0.78 g	1.11 g

Table 4 Comparison of Accelerations Acting on Containers

	Motions at Ship CG	Accelerations at Ship CG	Accelerations (m/s ²)			Accelerations (in g's)		
			(Maximum)	(Minimum)	Across-	(Maximum)	(Minimum)	Across-
			Normal- to-Deck	Normal- to-Deck	the-Deck	Normal- to-Deck	Normal- to-Deck	the-Deck
Bay 62 (aft-most bay) - 6th tier - outboard stack								
Surge (m - m/s ²)	-12.48	1.165						
Sway (m - m/s ²)	-2.27	0.221						
Heave (m - m/s ²)	1.57	-0.250			0.22			0.02
Roll (deg - rad/s ²)	-36.44	0.048	-0.25	-0.25	-1.14	-0.03	-0.03	-0.12
Pitch (deg - rad/s ²)	6.72	-0.027	0.65	-0.65		0.07	-0.07	
Yaw (deg - rad/s ²)	-5.08	0.002	-3.22	-3.22		-0.33	-0.33	
					-0.29			-0.03
Gravity Component without Wind effect			7.89	7.89	-5.83	0.80	0.80	-0.59
Gravity Component with 3.7 degr. Wind Heel			7.50	7.50	-6.32	0.76	0.76	-0.64
Total Acceleration			4.68	3.37	-7.54	0.48	0.34	-0.77

Table 5 Accelerations at Bay 62, 6th Tier, by MARIN Model Test

Analysis of the Container Securing System

Motion and acceleration data derived from the model tests and computer simulations were used to evaluate the lashing forces. For each stack, motions and accelerations are analyzed to determine the time when the loading on the container stack is

maximized. The lashings and containers are then evaluated in terms of lashing tension, racking, corner post compression and corner post tension.

Figure 36 and Figure 37 show the forces acting on a typical container stack aft. All containers are of equal weight and loaded to the limit of C11 lashing

criteria. The loads are shown as a percentage of the breaking strength of the individual components.

Figure 36 shows the loads on the containers and lashing pendant with the stack analyzed in accordance with the C11 lashing criteria. Corner-post tension is the governing constraint. The corner-post is loaded in tension to 75% of its breaking strength, which equals 100% of its design load.

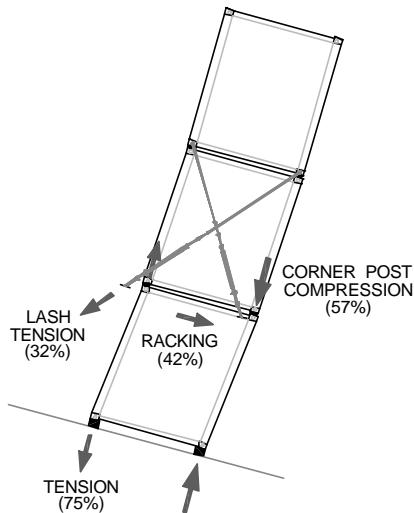


Figure 36 Loads into Containers and Lashings (when analyzed with C11 Lash Criterion)

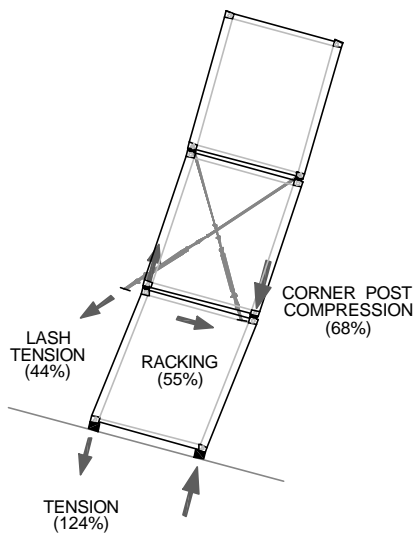


Figure 37 Loads into Containers and Lashings (when analyzed with model test data)

For Figure 37, the stack is analyzed by applying the accelerations derived from the model tests in short-crested head seas. The corner-post tension now increases from 75% to 124% of the breaking strength.

Failure of the first tier container and collapse of the container stack is likely, unless the particular container happens to have a tensile strength in excess of the assumed minimum breaking strength.

Analyses of each deck container stack on the vessel were carried out with accelerations based on (1) the MARIN model test no. 2310, (2) the LAMP numerical analysis, and, (3) the FREDYN numerical analysis. These all simulate the condition of the vessel during the storm encounter. For the model test and LAMP data, a wind heel angle of 3.7 deg was added to the maximum roll angle. In the case of FREDYN, the wind loads were directly applied during the analysis.

These analyses confirmed the expected failure of container stacks loaded to the C11 lashing criteria when the vessel was subject to head sea parametric rolling in the hindcast sea conditions.

Across-the-deck accelerations generated from the model tests are less than those predicted by numerical analysis. Therefore, at most stack locations the model test analysis produces the smallest loads into the containers and lashings. The LAMP predicted loads are typically about 10% higher than the model tests loads. The FREDYN results are somewhat higher, particularly for the midships and forward stacks.

Findings from Container Lashing Analysis

- a) Accelerations acting on deck stowed containers as computed from classification society rules vary significantly between societies. Therefore, the risk level associated with container stowage in accordance with the various rules is not consistent.
- b) When parametric rolling in head or near head seas, the combined effect of pitch and roll significantly increase loads on the containers and the securing system. The large roll motions generate high transverse (across-the-deck) accelerations. Simultaneously, large pitch motions introduce significant vertical (normal-to-deck) accelerations on the container stacks towards the bow and stern.
- c) When applying the motions and accelerations determined from the model test results for the hindcast seastate data, the increase in the loads on the containers were found to be sufficient to induce failure in stacks loaded to the C11 lashing design criteria.
- d) The model tests and time domain, nonlinear numerical simulations produced comparable results. The roll angles from the model tests were slightly less, and therefore the loads predicted by the simulations were higher (i.e. more conservative).

Findings and Recommendations

Summary of Findings

Parametric rolling in head seas was effectively simulated in the model tests, as well as through non-linear time domain analyses using the FREDYN and LAMP software systems. These studies confirmed that parametric rolling will occur when:

- the wave encounter period is approximately one-half the ship's natural roll period,
- the vessel is in head seas or near head seas,
- the wave damping is below a certain threshold level, and,
- the wave height is above a certain threshold level.

Vessels with flat transom sterns and significant bow flare are most prone to parametric rolling, due to the large variations in stability these vessels undergo in head and near head seas. Bow flare is also of importance due to the righting energy introduced at maximum roll angle, when the ship is pitched down by the head.

Stability diagrams developed for the Mathieu equation reveal that the bandwidth in which parametric roll can occur is quite broad when waterplane variations are sufficiently large and roll damping is relatively low. This susceptibility to parametric rolling was confirmed by both model tests and numerical analysis.

Model tests and nonlinear numerical simulation software such as the LAMP and FREDYN systems are well suited for investigating parametric roll on various ship types. The simulation tools effectively predict the conditions in which parametric rolling will occur and, when the speed and roll damping coefficients are tuned, produce responses that are in good agreement with model tests.

It was found that parametric rolling in head seas introduces loads into on-deck container stacks and their securing systems well in excess of those derived from classification society guidelines, or predicted through linear seakeeping analysis. The large roll amplitudes that are developed and the in-phase relationship of pitch and roll accelerations are of particular importance.

Evaluation of the actual load condition of the C11 class vessel in the hindcast seastate revealed that parametric rolling could be expected in these conditions. Both the model tests and LAMP analysis were carried out for short-crested seas based on the hindcast data, and the predicted roll responses from these investigations are consistent with those reported by the vessel's officers.

Recommendations

These studies and the events of late October 11th, 1998, demonstrate that head sea parametric rolling is a phenomenon that must be considered in the design and operation of certain vessels. The following recommendations are offered:

- a) Accelerations acting on deck stowed containers as computed from classification society rules vary significantly between societies. Therefore, the risk level associated with container stowage in accordance with the various rules is not consistent. The classification societies should work towards identifying an appropriate level of risk, and establishing more uniform guidelines. The rules should also be reviewed to insure that loadings on ship structure resulting from parametric rolling are properly accounted for.
- b) There is a need to make ship designers more aware of the phenomenon of head sea parametric rolling. This can be done through symposia, T&R bulletins and other technical publications.
- c) Designing container securing systems to withstand the forces induced by head sea parametric rolling will have major economic implications. Therefore, avoidance of head sea parametric rolling should be given careful attention during hull form development of future post-Panamax containerships.
- d) There is a need to educate vessel owners, operators, and merchant mariners concerning the phenomenon of head sea parametric rolling. This can be done through publications and seminars, as well as videos and instructional information specifically intended for shipboard personnel. Safe and unsafe combinations of heading and speed for various sea state / loading combinations should be identified and presented to the master. Such information can be made available in the form of polar plots or other diagrams, or included in the ship's motion monitoring and routing computer software.
- e) The IMO should consider enhancing MSC Circular 707, "Guidance to the Master for Avoiding Dangerous Situations in Following and Quartering Seas", to incorporate guidelines for operating vessels prone to head sea parametric rolling.
- f) Further research is needed to better understand the phenomenon of parametric rolling in head seas. For instance, parametric studies are needed to:

- Better understand the effects of hull form variations in general and bow flare in particular, to enable ship designers to optimize deck area while minimizing the risk of head sea parametric rolling.
- Determine the effects of variations in ship roll damping, including the effects of larger bilge keels as well as anti-roll tanks.
- Better define the range of headings and seastates, and the variations in wave encounter to roll period in which parametric rolling may occur.

In these regards, SNAME should consider establishing an Ad Hoc Technical and Research panel to foster further research, and to provide recommendations to naval architects and ship operators.

References

“ABS Guide for Certification of Container Securing Systems”, 1988.

Dallinga, R.P., Blik, J.J and Luth, H.R., “Excessive rolling of cruise ships in head and following waves”, RINA International Conference on ship Motions & Manoeuvrability. London, February 1998.

“Dalrymple Verification in the SMB”, WL/Delft hydraulics report nr. N3728, May 2000.

DeKat, J. O. and Paulling, J. R., “The Simulation of Ship Motions and Capsizing in Severe Seas”, *Transactions*, The Society of Naval Architects and Marine Engineers, vol. 97, 1989.

Dunwoody, A.B., “Roll of a ship in astern Seas – Metacentric height spectra”, *Journal of Ship Research* Vol 33, No. 3, September 1989, pp 221-228.

Dunwoody, A.B., “Roll of a ship in astern Seas – Response to GM fluctuations”, *Journal of Ship Research* Vol 33, No. 4, December 1989, pp 284-290.

Froude, William, “On the Rolling of Ships”, *The Papers of William Froude*, pub. By the Royal Institution of Naval Architects, London, 1955.

Graff, W. and E. Heckscher, "Widerstands und Stabilitäts versuche mit drei Fischdampfermodellen", *Werft-Reederei-Hafen*, vol. 22, 1941 (also DTMB Translation No.75, June 1942).

Haddara, M. R. , "On Nonlinear Rolling of Ships in Random Seas", *International Shipbuilding Progress*, Vol 20, 1973.

Hooft, J.P. "Mathematical Descripton of the Manoeuvrability of High Speed Surface Ships", MARIN report No. 47583-1-MOA, 1987.

IMO, “Guidance to the Master for Avoiding Dangerous Situations in Following and Quartering Seas”, MSC Circ. 707 dated 19 October 1995.

Kato, H., “Effect of Bilge Keels on the Rolling of Ships”, *Memories of the Defense Academy, Japan*, Vol. 4, 1966.

Kempf, G, "Die Stabilitätsbeanspruchung der Schiffe durch Wellen und Schwingungen", *Werft-Reederei-Hafen*, vol. 19, 1938.

Lin, W.M., and Salvesen, N., "Nine Years of Progress with LAMP – The Large Amplitude Motion Program", SAIC Report No. 97/1079, December 1998.

Luth, H.R. and Dallinga, R.P., “Prediction of excessive rolling of cruise vessels in head waves and following waves”, PRADS. The Hague Netherlands, 1998.

Meyers, W.G., Applebee, T.R. and Baitis, A.E., "User's Manual for the Standard Ship Motions Program, SMP", DTNSRDC/SPD-0936-01, September 1981.

Oakley, O. H., Paulling, J. R. and Wood, P. D. , “Ship Motions and Capsizing in Astern Seas”, *Proceedings*, Tenth ONR Symposium on Naval Hydrodynamics, ONR, ACR 204, 1974.

Oh, I., Nayfeh, A.H., Mook, D., “Theoretical and Experimental Study of the Nonlinearly Coupled Heave, Pitch, and Roll Motions of a Ship in Longitudinal Waves,” 19th Symposium on Naval Hydrodynamics, 1994.

Paulling, J. R. and Rosenberg, R. M., “On Unstable Ship Motions Resulting from Nonlinear Coupling”, *Journal of Ship Research*, vol 3, no.1, 1959.

Paulling, J. R. , “The Transverse Stability of a Ship in a Longitudinal Seaway”, *Journal of Ship Research*, vol. 4, no. 4, 1961.